A99-33709

AIAA 99-3758
INTER-WAKE TURBULENCE PROPERTIES IN HOMOGENEOUS PARTICLE-LADEN FLOWS

J.-H. Chen and G. M. Faeth
Department of Aerospace Engineering
The University of Michigan
Ann Arbor, Michigan 48109-2140

30th AIAA Fluid
Dynamics Conference
28 June - 1 July 1999/Norfolk, Virginia

INTER-WAKE TURBULENCE PROPERTIES IN HOMOGENEOUS PARTICLE-LADEN FLOWS

J.-H. Chen* and G. M. Faeth†
The University of Michigan, Ann Arbor, MI 48109-2140

Abstract

The properties of turbulence generated by uniform fluxes of monodisperse spherical particles moving through a uniform flowing gas were studied experimentally, emphasizing the properties of the region surrounding individual wake disturbances, i.e., the turbulent inter-wake region. Mean and fluctuating values, probability density functions and energy spectra of streamwise and cross stream velocities were measured within a counterflowing particle/air wind tunnel using particle wake discriminating laser velocimetry. Test conditions included nearly monodisperse glass spheres having diameters of 0.5-2.2 mm, particle Reynolds numbers of 106-990, mean particle spacings of 13-208 mm, particle volume fractions less than 0.003%, direct rates of dissipation of turbulence by particles less than 4%, and turbulence generation rates sufficient to yield streamwise relative turbulence intensities in the range 0.2-1.5%. The turbulent inter-wake region was homogeneous and nearly isotropic with probability density functions that are well approximated by Gaussian functions. Relative turbulence intensities were correlated effectively based on an analogy to the properties of isotropic grid-generated turbulence by scaling with the mean particle spacing normalized by the particle wake momentum diameter. For present turbulence generation conditions, the turbulent inter-wake region had turbulence Reynolds numbers of 0.4-3.5 and was in the final decay period where vortical regions fill the turbulent inter-wake region but are sparse. This implies enhanced rates of dissipation of turbulent kinetic energy, and decreasing macroscale/microscale ratios of the turbulence with increasing Reynolds numbers as opposed to increasing ratios with increasing Reynolds numbers typical of conventional fully-developed isotropic turbulence.

Nomenclature

A	=	dimensionless integral length scale, Eq. (10)
C_d	=	particle drag coefficient
D	=	dissipation factor, Eq. (7)
D_P	=	Parthasarathy dissipation factor, Eq. (8)
d_p	=	particle diameter
$E_u(k)$	=	streamwise energy spectrum
f	=	frequency
k	=	wave number, $2\pi/s$
K	=	kurtosis of PDF
L_u	=	streamwise integral length scale
ℓ_K	=	Kolmogorov length scale, $(\nu^3/\varepsilon)^{1/4}$
ℓ_p	=	mean particle spacing, Eq. (1)
M	=	mesh size of a grid
n	=	power in turbulence decay law, Eq. (4)
n″	=	particle number flux
PDF	=	probability density function
Re	=	particle Reynolds number, $d_p U_p/\nu$
Re_λ	=	turbulence Reynolds number, $Re_\lambda = \lambda \bar{u}'/\nu$
s	=	distance
S	=	skewness of PDF
t_K	=	Kolmogorov time scale, $(\nu/\varepsilon)^{1/2}$
U_p	=	mean streamwise relative velocity of a particle
u	=	streamwise gas velocity
u_K	=	Kolmogorov velocity scale, $(\varepsilon\nu)^{1/4}$
v	=	cross stream gas velocity
x	=	streamwise distance
x_o	=	streamwise virtual origin location
β	=	empirical coefficient, Eq. (5)
ε	=	rate of dissipation of turbulence kinetic energy
λ	=	Taylor length scale, Eq. (3)
ν	=	molecular kinematic viscosity of air
θ	=	wake momentum diameter, $(C_d d_p^2/8)^{1/2}$

Superscripts

$\bar{(\,)}$	=	mean value
$(\,)'$	=	r.m.s. fluctuating value
$\overline{(\,)'^2}$	=	mean square fluctuating value

*Graduate Student Research Assistant, Department of Aerospace Engineering.
†A.B. Modine Professor, Department of Aerospace Engineering, 1320 Beal Avenue, Fellow AIAA.

Introduction

Turbulence generation is the direct disturbance of the continuous-phase velocity field by the wakes of dispersed-phase objects in dispersed multiphase flows. Turbulence generation supplements the conventional production of turbulence due to mean velocity gradients in the continuous phase. Turbulence generation is most important when the dispersed-phase objects have large relative velocities (large Reynolds numbers) and relatively large relaxation times compared to characteristic turbulence times. Such conditions are typical of many practical dispersed multiphase flows having significant separated-flow effects, e.g., sprays, particle-laden jets, bubbly jets, rainstorms, etc. In spite of its importance, however, turbulence generation has not received much attention so that current understanding and capabilities for predicting its properties are very limited. Motivated by these observations, the objective of the present investigation was to extend past studies of turbulence generation in this laboratory, Refs. 1-3, to consider the properties of the continuous-phase region surrounding individual particle (drop) wake disturbances, i.e., the turbulent inter-wake region.

Earlier observations of flows resulting from turbulence generation in this laboratory have involved uniform fluxes of nearly monodisperse spherical particles moving at near terminal velocities in still water,[1] in still air,[2] and in upflowing air.[3] The resulting flows are homogeneous and stationary with turbulence production entirely due to turbulence generation. An interesting feature of these flows is that the local rate of dissipation of turbulence kinetic energy mainly controls continuous-phase turbulence properties and that this parameter is readily found as the local rate of loss of particle mechanical energy per unit volume (the particle dissipation rate). All other continuous-phase properties of the flow (moments, probability density functions, spectra, etc.), however, are not known and must be related to particle properties and particle dissipation rates.

The most recent study in this laboratory, involving particles in upflowing air,[3] avoided earlier problems of measurements in still environments that yielded flows having very large turbulence intensities.[1,2] It was found that relative turbulence intensities were proportional to the square root of the rate of dissipation in accord with a simplified stochastic theory of turbulence generation described in Refs. 1 and 2. Other properties, however, were not explained by the simplified stochastic theory and exhibited features not seen in conventional homogeneous turbulence: PDF's of streamwise velocities were not Gaussian whereas PDF's of cross stream velocities were Gaussian, and the energy spectra of both velocity components exhibited prominent -1 power decay regions in addition to the usual –5/3 power decay inertial region. These differences from conventional turbulence properties were attributed to effects of particle wakes that cannot be separated from other flow properties by conventional phase-discriminating velocity measurements because the arrival of particle wakes in these flows is random. Detailed observations, however, showed that particle wake properties approximated the properties of the laminar-like turbulent wakes observed for particle wakes at intermediate Reynolds numbers in conventional turbulent environments, described in Refs. 4-6, in spite of the unusual features of continuous-phase turbulence resulting from turbulence generation. Given estimates of the wake properties, it was subsequently shown that most practical turbulence generation processes involve particle wake disturbances surrounded by a relatively large turbulent inter-wake region.[7]

Stochastic analysis to estimate the overall properties of flows dominated by turbulence generation involves straightforward conditional averaging of the properties of the wake disturbances and the turbulent inter-wake region. At the present time, information is available concerning the laminar-like turbulent wake behavior of the wake disturbances,[5,6] and the overall properties of flows dominated by turbulence generation.[1-3] The missing element for predictions of the overall flow properties of turbulence generation involves information about the properties of the turbulent inter-wake region. Thus, the objectives of the present investigation were to complete conditional measurements of the properties of the turbulent inter-wake region for the range of conditions considered in Ref. 3, and to exploit existing methods in the turbulence literature to interpret and correlate the measurements.

Present measurements were carried out in a counterflow particle/air wind tunnel considering nearly monodisperse glass spheres having particle fluxes sufficient to yield relative turbulence intensities of 0.2-1.5%. Measurements were made using particle wake discriminating laser velocimetry to find moments and probability density functions of velocities, energy spectra of streamwise velocity fluctuations and characteristic time and length scales. These results were interpreted and correlated by studying potential analogies between the turbulent inter-wake region

of turbulence generation processes and homogeneous grid-generated turbulence, e.g., the studies of grid-generated turbulence of Refs. 8-12 and references cited therein. The present description of the study is brief, more details and a tabulation of the data can be found in Chen.[3]

Experimental Methods

The apparatus consisted of a vertical counterflow wind tunnel with upflowing air moving toward the suction side of the blower. and freely-falling particles introduced at the top of the wind tunnel using a particle feeder, see Ref. 3 for a complete description. The air flow path consisted of a rounded inlet, a flow straightener and a 16:1 contraction ratio to the 305 x 305 mm cross section windowed test section. The particle flow path consisted of a variable-speed particle feeder, a screen array particle dispersion section, a honeycomb particle flow straightener and a particle acceleration section to yield near terminal velocity particles at the test section. The particles were collected in a flexible plastic funnel below the air inlet.

Measurements included particle number fluxes by sampling and particle and gas velocities by a traversible laser velocimetry (LV) system. The particle measurements are described in Ref. 3; therefore, the following discussion will be limited to the gas velocity measurements. A single-channel, dual-beam, forward-scatter, frequency-shifted LV was used, based on the 514.5 nm line of an argon-ion laser. Streamwise and cross stream velocities were found by rotating the optics accordingly. A beam expander was used to yield a measuring volume diameter and length of 55 and 425 μm, respectively. The airflow entering the wind tunnel was seeded with oil drops having a 1 μm nominal diameter for the air velocity measurements. Velocities were found from the low-pass filtered analog output of a burst counter signal processor. The combination of frequency shifting plus a constant sampling rate of the analog output of the signal processor eliminated effects of directional bias and ambiguity and velocity bias. Due to small impaction efficiencies due to their small size, seeding particles were not collected by the glass spheres. Heavy seeding levels were used so that effects of LV step noise were deferred to scales roughly an order of magnitude larger than the Kolmogorov scales.

Conditional sampling was carried out by installing a particle detector so that disturbances from particle wakes could be deleted from the velocity record. The particle detection system consisted of a He-Ne laser sheet whose width was controlled by an adjustable slot. The sheet was observed through a laser line filter from a direction nearly normal to the path of the sheet, using another adjustable slot to control the length of the sheet that was observed. The LV measuring volume was positioned just below the He-Ne laser sheet at the center of the region observed. The required dimensions of the region of the laser sheet that was observed were estimated according to the laminar-like turbulent wake correlations of Refs. 5 and 6. The region included had a radius larger than twice the characteristic laminar-like wake radius (as defined in Refs. 5 and 6) from the particle wake axis. When strong scattering from a glass sphere was detected, velocity signals were not processed to contribute to the conditional properties of the turbulent inter-wake region for the time required for the particle wake to pass through the measuring plane. This time was selected so that the maximum mean velocity defect of the wake disturbance at the plane of the measurements was smaller than the velocity fluctuation level of the turbulent inter-wake region. Saturation of the particle detector occasionally allowed wake disturbances from a nearby particle to be recorded; such conditions were treated using velocity amplitude discrimination as discussed in Ref. 3. Finally, probability density functions of streamwise and cross stream velocities were used to access the effectiveness of the particle wake discrimination system as discussed later.

Velocity records having drop-out periods that resulted when disturbances due to particle wakes were removed were analyzed directly by correcting the sampling time for most velocity statistics, e.g., moments and other PDF properties. In contrast, obtaining correct temporal power spectra in the presence of dropout periods requires special treatment as described by Buchhave[13] and Buchave et al.[14], see Ref. 3 for the present application of these methods. Upflow velocities in the wind tunnel were set to provide absolute turbulence intensities less than 15% so that LV measuring conditions were excellent. Therefore, use of Taylor's hypothesis to convert measured temporal power spectra and scales to spatial spectra and scales is appropriate, see Hinze.[10] Sampling periods were adjusted to provide experimental uncertainties (95% confidence) less than 5% for mean velocities, less than 10% for rms velocity fluctuations, less than 10% for PDF's within one standard deviation of the most probable velocity and less than 20% for temporal power spectra at frequencies smaller than the reciprocal of the temporal integral scale with uncertainties smaller elsewhere.

Test conditions are summarized in Table 1. Particle properties were measured as described in Ref. 3. Assuming that the particles are falling randomly, the mean particle spacing is given by

$$\ell_p = ((U_p - \bar{u})/n'')^{1/3} \quad (1)$$

which yields values of 13-208 mm with corresponding particle volume fractions less than 0.003%. The direct dissipation of turbulence kinetic energy (dissipation) by particles was less than 4%; therefore; dissipation can be found from the rate of turbulence generation by particles, as follows:

$$\varepsilon = \pi n'' d_p^2 C_d U_p / 8 \quad (2)$$

Given ε, the Kolmogorov scales can be computed from their definitions. For these dissipation rates, relative turbulence intensities due to turbulence generation were in the range 0.2-5.0%. Measurements to be discussed later will show that inter-wake turbulence is similar to homogeneous isotropic turbulence so that Taylor's dissipation length scale can be estimated from the following equation:

$$\lambda = (15\nu \bar{u}'^2/\varepsilon)^{1/2} \quad (3)$$

Present values of λ are somewhat larger but comparable to Kolmogorov length scales (i.e., $\lambda/\ell_\kappa = 1.3\text{-}3.5$) which is not unexpected in view of the relatively small turbulence Reynolds numbers, 0.4-3.5, of the present turbulent inter-wake regions. Finally, streamwise integral length scales were obtained from energy spectra as discussed later, yielding values comparable to mean particle spacings, i.e., 11-178 mm.

Evaluation of the apparatus is discussed by Chen et al.[3] and Chen.[7] Measurements of particle number fluxes and phase velocities showed that they varied less than experimental uncertainties over the central 205 × 205 mm cross section of the flow, extending 200 mm in the streamwise direction, which surrounded the location where measurements were made. Similar measurements showed that flow properties varied less than experimental uncertainties as a function of time. Thus, present flows were properly homogeneous and stationary with turbulence within the turbulent inter-wake region produced by turbulence generation.

Results and Discussion

Relative Turbulence Intensities

Correlations of the properties of the turbulent inter-wake region were sought by drawing analogies between the turbulent inter-wake region and grid-generated turbulence. Past experimental observations show that turbulence downstream of grids can be divided into three regions: (1) a developing region near the grids, where the wakes from grid elements are merging and the turbulent flow is inhomogeneous and anisotropic; (2) an initial-decay region where the turbulent flow is nearly homogeneous and is locally isotropic; and (3) a final-decay region, where viscous effects dominate, and regions containing vorticity become sparse (giving the appearance of isolated turbulent spots from single-point measurements), and turbulence decays more rapidly than in the initial decay region. Thus, comparing the turbulent inter-wake region with grid-generated turbulence suggests that the wake disturbances of turbulence generation correspond to the developing region of grid-generated turbulence and that the turbulent inter-wake region of turbulence generation corresponds to either the initial- or final-decay regions of grid-generated turbulence. Batchelor and Townsend[11,12] suggest a value of $Re_\lambda \approx 5$ as the condition for the onset of the final-decay region for grid-generated turbulence; therefore, the present turbulent inter-wake regions involving $Re_\lambda \approx 0.4\text{-}3.5$ (see Table 1) have significant potential for behavior analogous to the final decay region.

The analogy between the present turbulent inter-wake region and grid-generated turbulence was based on an expression for grid-generated turbulence due to Batchelor and Townsend,[11,12] as follows:

$$(\bar{u}' \text{ or } \bar{v}')/\bar{u} = \beta(C_d M/(x-x_o))^n \quad (4)$$

where β is an empirical factor and they propose n = 1/2 and 5/4 in the initial- and final- decay periods, respectively. For present conditions, the turbulent inter-wake region was homogeneous; therefore, a reasonable analogy to the distance from the grid for grid-generated turbulence is a distance on the order of the mean particle spacing. The length corresponding to the product of mesh size and drag coefficient for grid-generated turbulence was taken to be the particle wake momentum diameter, θ, which similarly involves the product of the particle diameter and drag coefficient. Given these analogies, the expression corresponding to Eq. (4) for the turbulent inter-wake region becomes:

$$(\bar{u}' \text{ or } \bar{v}')/U_p = \beta(\theta/\ell_p)^n \quad (5)$$

where β may not necessarily be the same for $\overline{u}'$ and $\overline{v}'$. Introducing expressions for θ in terms of C_d and d_p, Eq. (1) for ℓ_p and eliminating n'' from the resulting expression using Eq. (2), yields the following potential correlation for the relative turbulence intensities of the turbulent inter-wake region:

$$(\overline{u}' \text{ or } \overline{v}')/U_p = \beta D^{n/3} \qquad (6)$$

where D is a dimensionless dissipation factor defined as follows:

$$D = (\theta/\ell_p)^3 = \varepsilon d_p (C_d/8)^{1/2}/(\pi U_p^2 (U_p - \overline{u})) \qquad (7)$$

During the earlier turbulence generation studies of Parthasarathy and coworkers,[1,2] expressions very similar to Eqs. (6) and (7) were developed that proved to be reasonably effective for correlating their relative turbulence intensity measurements. This expression was developed using a simple stochastic analysis to synthesize the properties of particle wake disturbances alone (with no consideration of a turbulent inter-wake region) based on Campbell's theorem, similar to the analysis of electrical noise due to Rice.[15] The resulting correlation was identical to Eq. (6) except that D was replaced by an alternative dimensionless dissipation factor, D_p, defined as follows:

$$D_p = \varepsilon d_p (C_d/8)^{1/3}/U_p^3 \qquad (8)$$

The dimensionless dissipation factors, D and D_p, are closely related for the stagnant flow conditions considered in Refs. 1 and 2 where $\overline{u} = 0$, noting that the effect of the different powers of C_d in Eqs. (7) and (8) is small because C_d is on the order of unity, see Table 1. Based on the measurements of Refs. 1 and 2, this correspondence between the two correlations suggests that n = 3/2. This estimate is reasonably close to the value n = 5/4 suggested by Batchelor and Townsend[11,12] where Eq. (4) is used to correlate turbulence intensities in the final-decay period of grid-generated turbulence, which is also consistent with the present relatively small values of Re_λ noted earlier.

Present measurement of streamwise and cross stream relative turbulence intensities, within the turbulent inter-wake region, for all three particle sizes, are plotted in Fig. 1 as a function of D according to Eq. (6). The correlation is seen to be remarkably good, over the two-order of magnitude range of D considered during the present experiments. Best fit correlations of the measurements found by linear regression had powers of 0.48 and 0.56 (with standard deviations of both these powers of 0.03) for streamwise and cross stream relative turbulence intensities, respectively. As a result, there is no statistical significance for the differences between the powers of these fits and the value of n = 3/2 found in Refs. 1 and 2. Thus, for consistency with this earlier work, the measurements were correlated as shown in Fig. 1 using the earlier value of n to yield

$$\overline{u}'/U_p = 9.2\, D^{1/2} \text{ and } \overline{v}'/U_p = 7.9\, D^{1/2} \qquad (9)$$

The standard deviation of the coefficients of Eqs. (9) are 1.5 and 1.6, respectively, and the correlation coefficients of both these fits are 0.98, which is excellent.

The difference between the coefficients of the streamwise and the cross stream relative turbulence intensities is not statistically significant. Thus, the turbulent inter-wake region is isotropic within present capabilities to evaluate this behavior. Slight anisotropy favoring the streamwise direction, however, is not unexpected. In particular, the present wake discrimination system was not totally effective as discussed later which introduces some streamwise velocity bias due to uneliminated streamwise mean velocity disturbances from wakes. In addition, past studies of grid-generated turbulence at small turbulence Reynolds numbers (Re_λ of 36-72 which is somewhat larger than the present range, see Table 1) due to Bennett and Corrsin[16] yielded values of $\overline{u}'/\overline{v}'$ in the range 1.09-1.22, which is similar to the present mean value of $\overline{u}'/\overline{v}' = 1.16$ found from Eqs. (9). Thus, potential for a small fundamental level of anisotropy for the turbulent inter-wake region cannot be ruled out.

The correspondence between the correlations of Eq. (6) involving D, based on sole consideration of the turbulent inter-wake region, and involving D_p, based on sole consideration of wake disturbances, helps explain the effectiveness of D_p for consideration the relative turbulence intensities observed in Refs. 1 and 2, even though the wake disturbance did not contribute significantly to these measurements (i.e., wake disturbances were largely eliminated by their phase-discrimination systems). Thus, the nearly identical definitions of D and D_p suggest that either approach is fortuitously appropriate for both the turbulent inter-wake and wake disturbance regions of flows caused by turbulence generation (even though the detailed properties of these two flow regions differ considerably).

Probability Density Functions

Potential departures of the turbulent inter-wake region from the behavior of isotropic turbulence were studied further by considering the probability density functions (PDF's) and the higher-order (skewness and kurtosis) statistical moments of streamwise and cross stream velocities. Typical measured streamwise and cross stream PDF's of velocities for various particle sizes and loadings are plotted in Figs. 2 and 3. Fits of the measurements are also shown on the plots, corresponding to best Gaussian fits based on rms velocity fluctuations. These PDF's are plotted using logarithmic scales in order to highlight potential effects of wake disturbances and the performance of the fits at the extremities of the distributions where the DPF's become small.

PDF's of cross stream velocities illustrated in Fig. 3 are symmetric which is consistent with absence of any preferred direction for cross stream velocities due to contributions from either the turbulent inter-wake region or from wake disturbances that were not completely eliminated by the wake discrimination system of the LV. The cross stream PDF's are also in generally good agreement with the Gaussian fits. The main exceptions are slight upward biases near both edges of the distributions which are thought to be due to increased experimental uncertainties near the extremities of the distributions due to sampling limitations (e.g., normalized PDF's at these locations are very small, on the order of 10^{-3}).

In contrast to the symmetric PDF's of cross stream velocities, the PDF's of streamwise velocities illustrated in Fig. 2 exhibit a distinct asymmetry. This involves an upward bias of the measurements from the Gaussian distribution near –2.5 standard deviations whereas the positive sides of the distributions agree quite well with Gaussian distributions. This behavior, however, no doubt results from small disturbances due to mean streamwise velocities in the particle wakes that were not eliminated by the present particle wake discrimination system.

Higher moments of the PDF's averaged over all the measurements in the turbulent inter-wake region, can be summarized as follows: values of S(u) and S(v) are –0.5 and 0.0, with standard deviations of 0.4 and 0.1, respectively; and values of K(u) and K(v) are 7 and 8, both with standard deviations of 2. The departure of measured values of skewness from the Gaussian value of S=0 are not statistically significant although the measurements do suggest a contribution of wake disturbances to the somewhat larger negative skewness of the PDF of streamwise velocities. The departure of the measured values of kurtosis from the Gaussian value of K=3 also borders on the limit of statistical significance, particularly in view of the larger experimental uncertainties of this high-order moment due to sampling limitations. Thus, the present PDF measurements within the turbulent inter-wake region are adequately described by Gaussian functions, similar to conventional isotropic turbulence.

Energy Spectra

Streamwise energy spectra within the turbulent inter-wake region were obtained using Taylor's hypothesis to transform measured temporal spectra to spatial spectra as described previously. The corresponding integral length scales were found by noting that the normalized amplitude of the energy spectra plots, $2\pi E_u(k)/(\bar{u}'^2 L_u)$, approaches the value of 4 as the normalized wave number of these plots, $kL_u/(2\pi)$, becomes small, analogous to temporal spectra as discussed by Hinze.[10] The resulting normalized energy spectra of streamwise velocity fluctuations are illustrated in Fig. 4 for various particle sizes and loadings. Correlations of energy spectra for approximate isotropic turbulence are also shown on the plot for comparison with the measurements. The approximate spectra represent the simplification of isotropic turbulence discussed by Hinze,[10] where correlations of velocity fluctuations are assumed to satisfy exponential functions. This simplification implies that the –5/3 power decay of the energy spectra within the inertial subrange of turbulence is approximated by a –2 power decay.

Although the energy spectra illustrated in Fig. 4 are separated by particle sizes to help readability, the spectra are independent of both particle size and loading and agree reasonably well with the isotropic turbulence approximation described by Hinze.[10] Thus, the prominent –1 power decay region of the spectra of the overall flow (wake disturbances plus the turbulent inter-wake region) of continuous-phase turbulence resulting from turbulence generation, seen in Refs. 1-3, disappears when the particle wake disturbances are removed. This finding implies that the –1 power decay region seen for the overall flow is caused by wake disturbances. Finally, the present spectra are truncated at large wave numbers to avoid step noise caused by sampling limitations, with full spectra expected to reach wave numbers characteristic of Kolmogorov scales at values of $kL_u/(2\pi)$ on the order of 100. Thus, the present inter-wake turbulence exhibits a substantial range of scales, roughly 1000:1, even though turbulence Reynolds numbers are small, less than 4. Consideration of length scales in the present

turbulent inter-wake regions, however, will show that the present large range of scales represent reasonable behavior for turbulence in the final decay period which is characteristic of the turbulent inter-wake region for present test conditions. These same considerations of length scales will also show that the present large range of scales appears for very different reasons than in high Reynolds number isotropic turbulence. This behavior will be discussed next.

Length Scales

Numerous studies of isotropic turbulence at large turbulence Reynolds numbers show that the rate of dissipation of turbulence kinetic energy can be estimated from values of velocity fluctuations and integral length scales using the following equation:[10]

$$A = \varepsilon L_u/(\overline{u}')^3 \qquad (10)$$

where A, the dimensionless integral length scale, is believed to be a constant on the order of unity. All properties on the right hand side of Eq. (10) have been measured during the present investigation so that values of A can be found at much smaller Re_λ than considered in the past.

The resulting values of A from the present investigation are plotted as a function of Re_λ in Fig. 5, providing results at small Reynolds numbers, Re_λ = 0.4-3.5. Results for isotropic turbulence from several past experiments,[17-21] and from direct numerical simulations (DNS),[22-25] along with a DNS data fit due to Sreenivasan,[26] are plotted along with the present measurements. The earlier determination of A involve relatively large turbulence Reynolds numbers, $20 \le Re_\lambda \le 800$, which places these flows in the initial decay period of isotropic turbulence where the turbulence is fully developed and acts over the entire flow region similar to conventional turbulence. In contrast, present measurements at small values of Re_λ exhibit very enhanced rates of dissipation, which is typical of behavior in the final decay period where the vorticity is sparse and turbulence appears to involve disconnected spots when single-point measurements are observed.[4,11,12,27,28] This behavior is also consistent with previous indications that inter-wake turbulence was in the final decay period, based on relative turbulence intensities as discussed in connection with Fig. 1.

The measurement and predictions at large Re_λ yield scattered values of A in the range 0.3-2.0 which are on the order of unity and independent of Re_λ, as expected. Sreenivasan[26] suggests that these variations of A are due to different initial conditions or grid geometries of the flows that were considered. In contrast, present values within the final decay period indicate strongly enhanced dissipation as Re_λ decreases (indicated by increasing values of A), analogous to strongly enhanced dissipation as Re_λ decreases (indicated by decreasing values of the turbulence intensity) along the axis of turbulent wakes in the final decay period, see Ref. 4. The present measurements of A within the final decay period yield a best fit correlation as follows:

$$A = 1130\ Re_\lambda^{-2.33};\ 0.4 \le Re_\lambda \le 3.5 \qquad (11)$$

where the experimental uncertainty of the power of Re_λ is 0.16 and the correlation coefficient of the fit is 0.96. Combining all the observations of A illustrated in Fig. 5, it is evident that A exhibits three regimes: (1) a large Re_λ regime (the initial-decay period) with $Re_\lambda > 100$, which corresponds to classical homogeneous isotropic turbulence at large Reynolds numbers; (2) a small Re_λ regime (the final-decay period) where $Re_\lambda < 10$, which corresponds to present turbulent inter-wake conditions; and (3) a transition regime with $10 < Re_\lambda < 100$, between the two outer limiting regimes.

It is interesting to consider the variation of the length scale ratio, L_u/λ, as a function of Re_λ, in the three regimes of A that were just defined. It is easy to show that this ratio assumes the following forms:

Final-decay period:

$$L_u/\lambda = 75\ Re_\lambda^{-1.33};\ 0.4 \le Re_\lambda \le 3.5 \qquad (12)$$

Initial-decay period:

$$L_u/\lambda = A\ Re_\lambda/15,\ 20 \le Re_\lambda \qquad (13)$$

Finally, in the transition region, Ling and Huang find $A \sim Re_\lambda^{-1}$, which implies:

Transition period:

$$L_u/\lambda = 2.2,\quad 4 \le Re_\lambda \le 20 \qquad (14)$$

The correlations of Eqs. (12)-(14) are illustrated in Fig. 6,. along with results from available measurements and DNS simulations. Taken together, the various correlations provide reasonably good fis of results in the final-decay, transition and initial-decay periods.

The nature and location of transition to the final decay period seen in Fig. 6 seems quite reasonable. In particular, the variation of L_u/λ with decreasing Re_λ for fully-developed turbulent flows must change as Re_λ becomes small because realizable flow properties cannot involve a Taylor length scale (a microscale) larger than the integral scale (a macroscale), or conditions where $L_u/\lambda_\lambda < 1$. Thus, it is not surprising that the transition to the final-decay period, where L_u/λ_λ increases with decreasing Re_λ, occurs when L_u/λ reaches values on the order of unity.

Increasing values of L_u/λ with *increasing* Re_λ in the initial-decay period is well understood,[8,10] as a result of the relatively inviscid large-scale features (on the scale of integral scales) combined with progressively smaller microscales of turbulence as turbulence Reynolds numbers increases. The corresponding increasing values of L_u/λ with *decreasing* values of Re_λ in in the final-decay period occurs for very different reasons. In this case, vortical regions are sparse although they still spread throughout the entire flow, yielding large integral scales in the presence of small dissipation scales; i.e., the dimensions of turbulent spots become small in comparison to the dimensions of the flow as a whole when the vortical regions of the flow become more sparse as turbulence decay proceeds.

Conclusions

This investigation considered the properties of turbulence generated by uniform fluxes of monodisperse spherical particles moving through air at standard temperature and pressure, emphasizing the properties of the turbulent inter-wake region. Test conditions included nearly monodisperse glass beads having diameters of 0.5-2.2 mm, particle Reynolds numbers of 106-990, mean particle spacings of 13-208 mm, particle volume fractions less than 0.003%, direct rates of dissipation of turbulence by particles less than 4%, and turbulence generation rates sufficient to yield streamwise relative turbulence intensities of 0.2-1.5%. The major conclusions of the study are as follows:

1. The turbulent inter-wake region is homogeneous and nearly isotropic with probability density functions of streamwise and cross stream velocities well approximated by Gaussian functions.
2. Relative turbulence intensities in the turbulent inter-wake region were correlated effectively by analogy to the known properties of isotropic grid-generated turbulence, e.g., Batchelor and Townsend,[11,12] by scaling these properties with the mean particle spacing normalized by the particle wake momentum diameter, to yield a dimensionless dissipation factor.
3. The present dimensionless dissipation factor, based on consideration of inter-wake turbulence alone, is nearly identical to an earlier dimensionless dissipation factor found in Refs. 1 and 2, based on consideration of particle wake properties alone. This fortuitous agreement of correlations for the turbulent inter-wake region and for wake disturbances is no doubt responsible for the simple correlations of overall relative turbulence intensities (involving both regions) as a function of dimensionless dissipation factor observed during earlier work, see Refs 1-3.
4. For present turbulence generation conditions, and probably for most practical dispersed flows, the turbulent inter-wake region exhibited very small turbulence Reynolds numbers ($Re_\lambda<4$) and was in the final decay period where vortical regions fill the entire inter-wake region but are sparse, i.e., where turbulence appears to involve disconnected turbulent spots when single-point measurements are observed.
5. Within the final decay period, macroscale/microscale ratios (e.g., L_u/λ) decrease with increasing turbulence Reynolds numbers as opposed to increasing similar to fully-developed isotropic turbulence at large turbulence Reynolds numbers. Quite plausibly, the transition from the final decay region to the fully-developed turbulence region occurs when L_u/λ is on the order of unity; this condition corresponds to a turbulence Reynolds number on the order of ten which is similar to conditions at the transition of turbulent wakes in nonturbulent environments to the final decay period, see Ref. 4.

Acknowledgments

This investigation was supported by the Air Force Office of Scientific Research, Grant Nos. F49620-92-J-0399 and F49620-95-1-0364, under the technical management of J.M. Tishkoff. The U.S. Government is authorized to reproduce and distribute copies of the paper for governmental purposes notwithstanding any copyright notation therein.

References

[1]Parthasarathy, R.N., and Faeth, G.M., "Turbulence Modulation in Homogeneous Dilute Particle-Laden Flows," J. Fluid Mech., Vol. 220, Pt.2, 1990, pp. 485-514.

[2]Mizukami, M., Parthasarathy, R.N., and Faeth, G.M., "Particle-Generated Turbulence in Homogeneous Dilute Dispersed Flows," Int. J. Multiphase Flow, Vol. 18, No. 2, 1992, pp. 397-412.

[3]Chen, J.-H., Wu, J.-S., and Faeth, G.M., "Turbulence Generation in Homogeneous Particle-Laden Flows," AIAA J., submitted.

[4]Wu, J.-S., and Faeth, G.M. "Sphere Wakes in Still Surroundings at Intermediate Reynolds Numbers," AIAA J., Vol. 31, No. 8, 1993, pp. 1448-1455.

[5]Wu, J.-S., and Faeth, G.M., "Sphere Wakes at Moderate Reynolds Numbers in a Turbulent Environment," AIAA J., Vol. 32, No. 3, 1994, pp. 535-541.

[6]Wu, J.-S., and Faeth, G.M., "Effects of Ambient Turbulence Intensity on Sphere Wakes at Intermediate Reynolds Numbers," AIAA J., Vol. 33, No. 1, 1995, pp. 171-173.

[7]Chen, J.-H., "Turbulence Generation in Homogeneous Dilute Particle-Laden Flows," Ph.D. Thesis, Department of Naval Architecture and Marine Engineering, Univ. of Michigan, Ann Arbor, MI, 1999.

[8]Schlichting, H., *Boundary Layer Theory*, 7th Ed., McGraw-Hill, New York, 1979, pp. 234-235 and 599.

[9]Tennekes, H., and Lumley, J.L., *A First Course in Turbulence*, MIT Press, Cambridge, Massachusetts, 1972, pp. 113-124 and 196-201.

[10]Hinze, J.O., *Turbulence*, 2nd Ed., McGraw-Hill, New York, 1975, Chapt. 3, and pp. 65-67, 204, 496-519.

[11]Batchelor, G.K., and Townsend, A.A., "Decay of Isotropic Turbulence in the Initial Period," Proc. Roy. Soc. (London), Vol. A193A, 1948, pp. 539-558.

[12]Batchelor, G.K., and Townsend, A.A., "Decay of Turbulence in the Final Period," Proc. Roy. Soc. (London), Vol. 194A, 1948, pp. 527-543.

[13]Buchhave, P., "The Measurement of Turbulence with the Burst-Type Laser Doppler Anemometer--Errors and Correction Methods," Ph.D. Thesis, Department of Mechanical and Aerospace Engineering, State University of New York at Buffalo, Buffalo, NY, 1979.

[14]Buchhave, P., George, W.K., and Lumley, J.L., "The Measurement of Turbulence with the Laser-Doppler Anemometer," Ann. Rev. Fluid Mech., Vol. 11, 1979, pp. 443-504.

[15]Rice, S. O., "Mathematical Analysis of Random Noise," *Noise and Stochastic Processes* (N. Wax, ed.), Dover Publications, New York, 1954, pp. 133-294.

[16]Bennett, J.C., and Corrsin, S., "Small Reynolds Number Nearly Isotropic Turbulence in a Straight Duct and a Contraction," Phys. Fluids, Vol. 21, 1978, pp. 2129-2140.

[17]Kistler, A.L., and Vrebalovich, T., "Grid Turbulence at Large Reynolds Numbers," J. Fluid Mech., Vol. 26, Pt. 1, 1966, pp. 37-47.

[18]Comte-Bellot, G., and Corrsin, S., "Simple Eulerian Time Correlation of Full-and Narrow-Band Velocity Signals in 'Grid-Generated', Isotropic Turbulence," J. Fluid Mech., Vol. 48, 1971, pp. 273-337.

[19]Mohamed, M.S., and La Rue, J.C., "The Decay Power Law in Grid-Generated Turbulence," J. Fluid Mech., Vol. 219, 1990, pp. 195-214.

[20]Tong, C., and Warhaft, Z., "On Passive Scalar Derivative Statistics in Grid Turbulence," Phys. Fluids, Vol. 6, 1994, pp. 2165-2176.

[21]Mydlarski, L., and Warhaft, Z., "On the Onset of High-Reynolds-Number Grid-Generated Wind Tunnel Turbulence," J. Fluid Mech., Vol. 320, 1996, pp. 331-368.

[22]Jiminez, J., Wray, A.A., Saffman, P.G., and Rogallo, R.S., "The Structure of Intense Vorticity in Isotropic Turbulence," J. Fluid Mech., Vol. 255, 1993, pp. 65-90.

[23]Wang, L.-P., Chen, S., Brasseur, J.G., and Wyngaard, J.C., "Examination of Hypotheses in the Kolmogorov Refined Turbulence Theory Through High-Resolution Simulations, Part I Velocity Field," J. Fluid Mech., Vol. 309, 1996, pp. 113-156.

[24]Yeung, P.K., and Zhou, Y., "On the Universality of the Kolmogorov Constant in Numerical Simulation of Turbulence," Phys. Rev. E, Vol. 18, 1997, pp. 1746.

[25]Cao, N., Chen, S., and Doolen, G.D., "Statistics and Structure of Pressure in Isotropic Turbulence," cited by Sreenivasan.[26]

[26]Sreenivasan, K.R., "An Update on the Energy Dissipation Rate in Isotropic Turbulence," Phys. Fluids, Vol. 10, 1998, pp. 529.

[27]Ling, S.C., and Huang, T.T., "Decay of Weak Turbulence," Phys. Fluids, Vol. 13, 1970, pp. 2912-2924.

[28]Phillips, O.M., "The Final Period of Decay of Non-Homogeneous Turbulence," Proc. Cambridge Phil. Soc., Vol. 52, 1956, pp. 135-151.

Table 1. Summary of Test Conditions[a]

Nominal Particle Diameter (mm)	0.5	1.1	2.2
U_p (mm/s)	3370	5530	7000
Re (-)	106	373	990
C_d(-)	1.22	0.79	0.54
θ (mm)	0.183	0.299	0.519
n"(kpart/m^{2}s)	71-950	4-56	0.5-10
ℓ_p(mm)	13-32	41-97	77-208
ε (m^2/s^3)	0.088-1.17	0.041-0.54	0.012-2.3
ℓ_K (mm)	0.2-0.5	0.3-0.6	0.4-0.7
t_K (ms)	4-14	5-16	8-37
u_K (mm/s)	34-60	31-54	21-44
$\overline{u}'/U_p$ (%)	0.5-1.5	0.2-0.6	0.2-0.6
λ (mm)	0.7-0.9	0.6-0.8	1.2-1.8
Re_λ (-)	0.7-2.5	0.4-1.5	1.4-3.5
L_u(mm)	11-35	42-178	23-156

[a] Round glass beads (density of 2500 kg/m^3) falling in upflowing air at standard temperature and pressure (air density of 1.16 kg/m^3 and kinematic viscosity of 15.9 mm^2/s) having a mean velocity of 1.1 m/s.

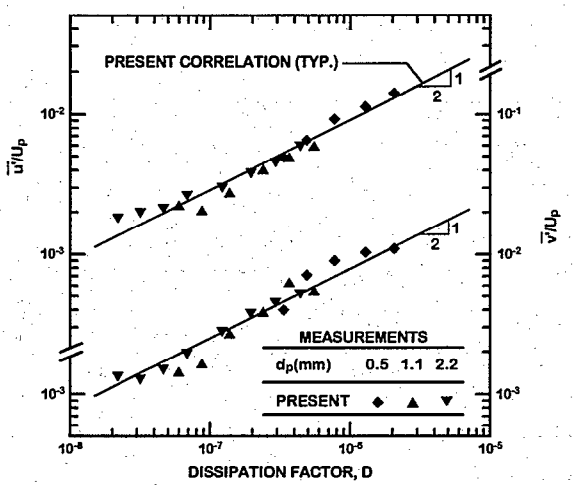

Fig.1 Streamwise and cross stream relative turbulence intensities as a function of the dissipation factor for various particle sizes.

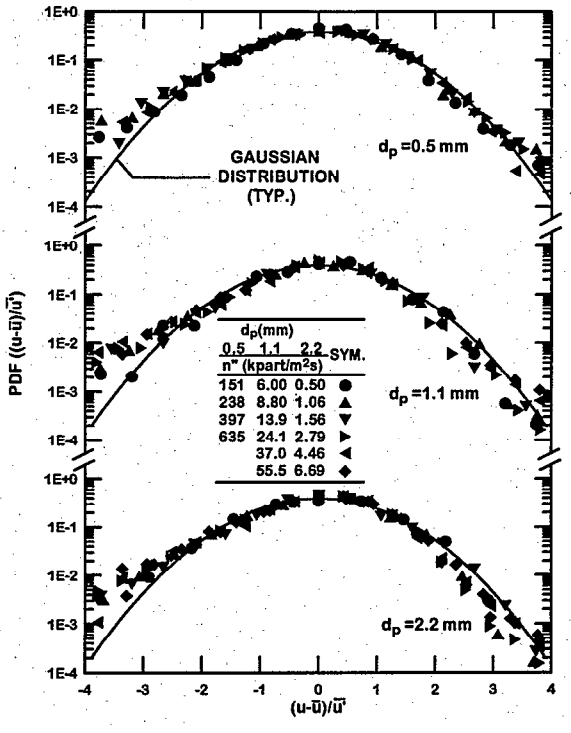

Fig.2 Typical PDF's of streamwise velocities for various particle sizes and number fluxes.

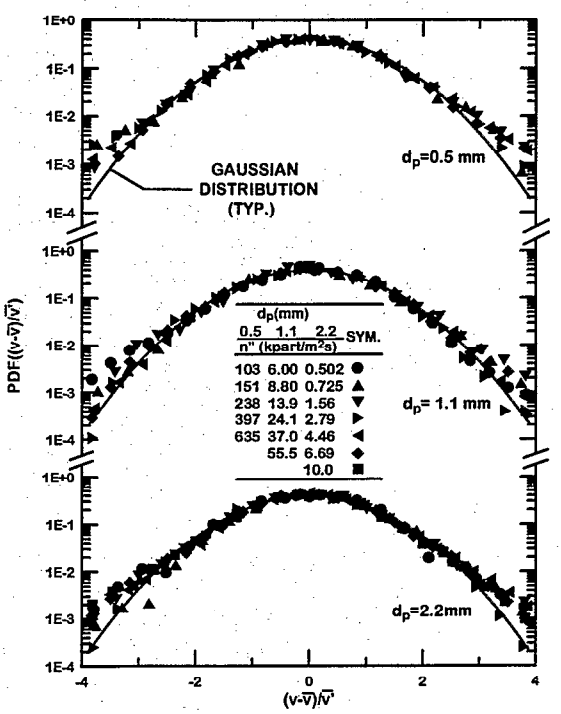

Fig.3 Typical PDF's of cross stream velocities for various particle sizes and number fluxes.

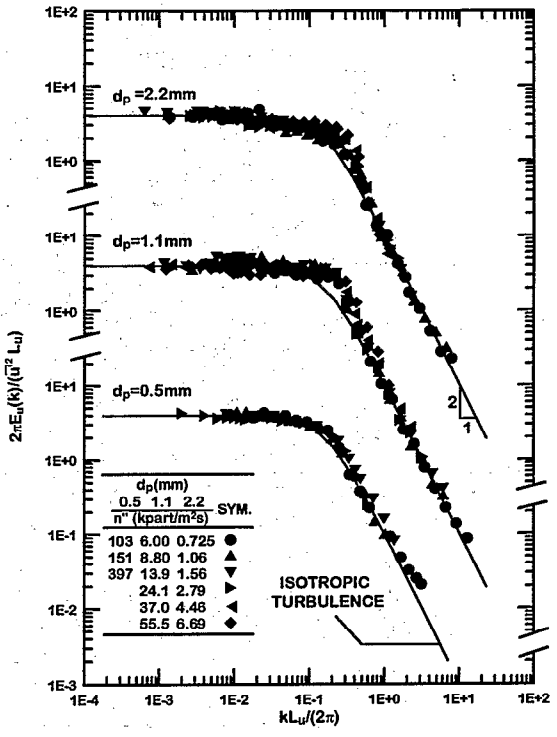

Fig. 4 Energy spectra of streamwise velocity fluctuations for various particle sizes and number fluxes.

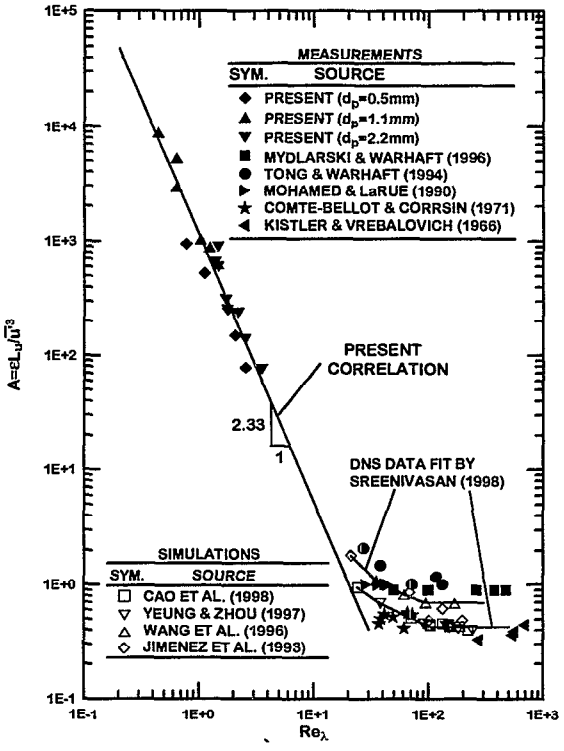

Fig.5 Normalized integral length scales as a function of turbulence Reynolds number for both grid-generated and particle-generated turbulence. Measurements of Kistler and Vrebalovich,[17] Comte-Bellot and Corrsin,[18] Mohamed and LaRue,[19] Tong and Warhaft,[20] Mydlarski and Warhaft[21] and the present investigation; predictions of Jiminez et al.,[22] Wang, et al.,[23] Yeung and Zhou[24] and Cao et al.;[25] DNS data fit of Sreenivasan.[26]

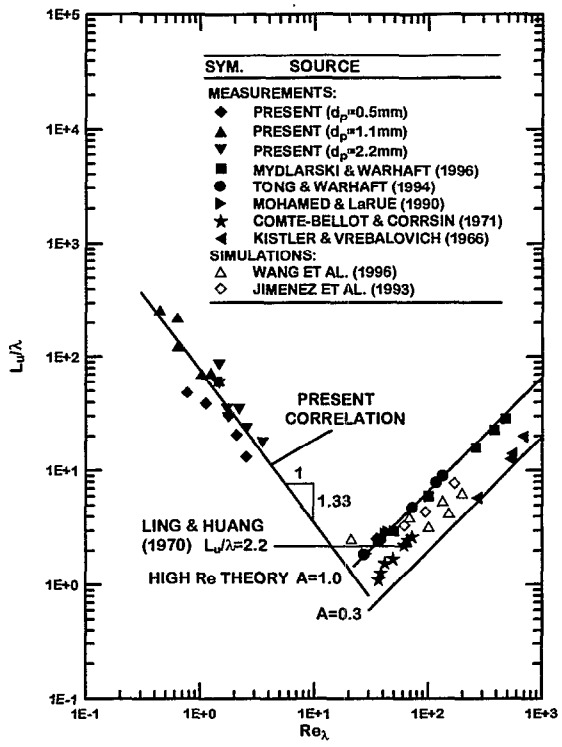

Fig.6 Ratios of integral and Taylor length scales as a function of turbulence Reynolds number for both grid-generated and particle-generated turbulence. Measurements of Kistler and Vrebalovich,[17] Comte-Bellot and Corrsin,[18] Mohamed and LaRue,[19] Tong and Warhaft,[20] Mydlarski and Warhaft[21] and the present investigation; predictions of Jiminez et al.[22] and Wang et al.;[23] correlation of Ling and Huang.[27]